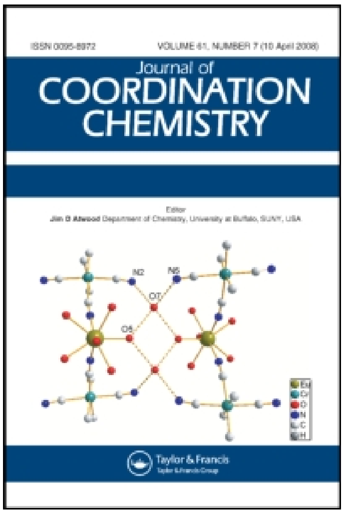

**Journal of Coordination Chemistry**
Publication details, including instructions for authors and subscription information:
http://www.informaworld.com/smpp/title~content=t713455674

# Synthesis, crystal structures and properties of five-coordinate Schiff-base Zn(II) complexes

D. Zhu[a]; Z. Su[a]; Z. Mu[a]; Y. Qiu[a]; Y. Wang[a]
[a] Department of Chemistry, Institute of Functional Materials, Northeast Normal University, Jilin, PR China

**To cite this Article** Zhu, D. , Su, Z. , Mu, Z. , Qiu, Y. and Wang, Y.(2006) 'Synthesis, crystal structures and properties of five-coordinate Schiff-base Zn(II) complexes', Journal of Coordination Chemistry, 59: 4, 409 — 419
**To link to this Article: DOI:** 10.1080/00958970500270877
**URL:** http://dx.doi.org/10.1080/00958970500270877

*Journal of Coordination Chemistry*
Vol. 59, No. 4, March 2006, 409–419

Taylor & Francis
Taylor & Francis Group

# Synthesis, crystal structures and properties of five-coordinate Schiff-base Zn(II) complexes

D. ZHU†, Z. SU†, Z. MU†, Y. QIU† and Y. WANG*‡

†Department of Chemistry, Institute of Functional Materials, Northeast Normal University,
Changchun, Jilin, 130024, PR China
‡Key Laboratory for Supramolecular Structure and Materials of Education,
Jilin University, Changchun, Jilin, 130023, PR China

(*Received in final form 18 July 2005*)

Five-coordinate Schiff-base Zn complexes (1,2-cyclohexanediamino-N,N′-bis(salicylidene)) zinc-pyridine **1** and (1,2-cyclohexanediamino-N,N′-bis(3,5-di-tert-butylsalicylidene)) zinc-pyridine **2** were synthesized and the structures of **1** and **2** have been determined by single-crystal X-ray analysis. All Zn atoms are five-coordinate in both structures. Both complexes exhibit interesting structures based on intermolecular $\pi$–$\pi$ stacking and hydrogen bond interactions. Complex **1** has a one-dimensional molecular chain structure via $\pi$–$\pi$ stacking interaction, while complex **2** has an interesting lattice structure (with cavities with dimensions $10.9 \times 6.9$ Å) formed through intermolecular $\pi$–$\pi$ stacking and hydrogen bond interactions. **1** and **2** are compared and characterized by MS, elemental analysis, IR, UV-Vis and Photoluminescence (PL). Fluorescence spectra show that the maximal emission wavelength of **1** and **2** are 454 nm, and 480 nm, respectively, upon radiation by UV light. Cyclic voltammetry performed on **1** and **2** indicate a dependence of the cathodic potentials upon conformational and electronic effects. Electronic spectral properties of **1** and **2** were studied by TD-DFT methods. The fluorescent emission of these complexes originates from ligand-centred $\pi$–$\pi^*$ transitions. The Zn (II) centres play a key role in enhancing the fluorescent emission of the ligands.

*Keywords*: Crystal structure; Schiff-base complexes; Five-coordinate complexes; Cyclic voltammetry; TD-DFT

## 1. Introduction

Hugo Schiff described the condensation between an aldehyde and an amine leading to a Schiff base in 1864 [1]. Schiff-base ligands coordinate metals through imine nitrogen and other groups, usually linked to the aldehyde [2–4]. Active and well-designed Schiff-base ligands are considered ‘privileged ligands’, because of their wide application in the fields of synthesis and catalysis [5]. Attention is still growing, with considerable

---

*Corresponding author. Fax: +86-431-5684009. Email: zmsu@nenu.edu.cn

*Journal of Coordination Chemistry*
ISSN 0095-8972 print: ISSN 1029-0389 online
DOI: 10.1080/00958970500270877

research devoted to the synthesis of new Schiff-base complexes with transition and main group metal ions, to further develop applications in both catalysis and materials chemistry [6–11]. The salicylaldimine ligand forms the basis of an extensive class of chelating ligands that has enjoyed popular use in the coordination chemistry of transition and main group elements [12].

Metal complexes of Schiff bases have been under investigation for many years due to their striking structural features and their biological activities [13–17], as some of the metal complexes have anticancer activity [18–20]. The structures of salicylaldehyde Schiff bases are similar to those of 8-hydroxyquinoline and 10-hydroxybenzo[*h*]quinoline ligands, in which both have at least one hydroxyphenyl moiety, a coordination nitrogen atom, and a delocalized $\pi$-system [12]. However, the structures of salicylaldehyde Schiff bases are certainly more flexible than those of 8-hydroxyquinoline. Tris (8-hydroxyquinolinato) aluminum (Alq3) [21] and bis (10-hydroxyben-zo[*h*]quinolinato)beryllium (Bebq2) [22] have excellent properties as electroluminescent (EL) materials, such as good charge transport, highly stable film formation, and good heat resistance. Metal complexes of salicyladehyde Schiff-base ligands are expected to show good luminescent properties, our goal in searching for new organic electroluminescence (OEL). Little has been achieved in the formation of complexes between the salicylaldehyde Schiff-base ligands and zinc, perhaps attributed to the fact that neutral Salen complexes are generally insoluble in common solvents [23]. The present paper deals mainly with the syntheses, X-ray crystal analysis, absorption and fluorescence spectra, electrochemical studies and absorption spectra calculation with TD-DFT methods for five-coordinate Zn complexes.

## 2. Experimental

### 2.1. *Materials and methods*

The 1,2-diaminocyclohexane, salicylaldehyde and 3,5-di-tert-butyl-hydroxybenzaldehyde were purchased from Sigma and used without further purification. All other reagents and solvents were purchased from commercial sources and were analytical grade.

Mass spectra were measured on a JEOL Mod. JMS-SX-102A spectrometer. Elemental analyses were performed on a Perkin-Elmer 240C elemental analyser. The IR spectra were recorded on KBr discs on a Nicolet Magna560 spectrophotometer in the 400–4000 $cm^{-1}$ region. The UV-Vis spectra were recorded with a Varian Cary 500 UV-Vis spectrophotometer. Luminescent spectra were measured on a RF-5000 Fluorimeter. The cyclic voltammograms were recorded with a Chen Hua CHI 610 electrochemical system. All theoretical calculations were carried out with the Gausssian 98 program package and the absorption spectra were obtained with the TD-DFT method [24].

### 2.2. *Preparation of complexes*

**2.2.1. (1,2-cyclohexanediamino-N, N′-bis (salicylidene) zinc-pyridine, chsa-Zn-pyridine.** The ligand chsa was prepared from reaction of 1,2-diaminocyclohexane with salicylaldehyde. The ligand chsa coordinated with $Zn^{2+}$ giving chsa-Zn. In a 100 mL round-bottom flask fitted with magnetic stirrer, $Zn(Ac)_2 \cdot 2H_2O$(1.09 g,5 mmol) and 30 mL of methanol were slowly added to chsa (1.61 g, 5 mmol) in 30 mL of methanol. The resulting solution was stirred and refluxed for 3 h. Yellow solid precipitated from the solution was collected by filtration and purified by recrystallization and sublimation methods. Suitable X-ray quality crystals of **1** were grown by slow layer diffusion of ether into a saturated pyridine solution of chsa-Zn at room temperature. EIMS: $m/z = 465$. Anal. Calcd. For $C_{25}H_{25}N_3O_2Zn$: C. 64.94%; H. 4.98%; N. 9.09%; O. 6.93%; Zn. 14.07%. Found: C. 64.97%; H. 4.4.97%; N. 9.07%; O. 6.95%; Zn. 14.05%. FT-IR (KBr pellet, $cm^{-1}$): 3146m, 2930w, 2856m, 1600m ($\nu_{C=N}$), 1534s, 1601s, 1543m, 1467w, 1243s, 1019m, 906m.

**2.2.2. (1,2-cyclohexanediamino-N,N′-bis(3,5-di-tert-butylsalicylidene)) zinc-pyridine, chsa$^t$(Bu)-Zn-pyridine.** The same procedure as for chsa-Zn was used with chsa$^t$(Bu) (2.72 g, 5 mmol) in 30 mL of methanol, and $Zn(Ac)_2 \cdot 2H_2O$ (1.09 g, 5 mmol) in 30 mL of methanol. chsa($^t$Bu)-Zn was dissolved in pyridine and the pyridine was allowed to evaporate slightly, forming suitable X-ray quality crystals of **2**.

EIMS: $m/z = 690$. Anal. Calcd. For $C_{41}H_{57}N_3O_2Zn$: C. 71.72%; H. 8.02%; N. 6.12%; O. 4.66%; Zn. 9.48%. Found: C. 71. 69%; H. 8.05%; N. 6.08%; O. 4.70%; Zn. 9.52%. FT-IR (KBr pellet, $cm^{-1}$): 3046m, 2955w, 2866m, 1616s ($\nu_{C=N}$), 1550m, 1454w, 1253s, 1041m, 874m.

### 2.3. *X-ray crystallography*

Single crystals of **1** and **2** with dimensions $0.21 \times 0.12 \times 0.08\,mm^3$ and $0.66 \times 0.08 \times 0.04\,mm^3$, respectively, were glued on a glass fiber. Data were collected on a Rigaku R-AXIS RAPID IP diffractometer with Mo K$\alpha$ monochromated radiation ($\lambda = 0.71073$ Å) at 293K. An empirical absorption correction was applied. The structures were solved by the direct method and refined by the full-matrix least-squares on $F^2$ using the SHELXTL crystallographic software package [25]. Anisotropic thermal parameters were used to refine all non-hydrogen atoms. Hydrogen atoms were located from difference Fourier maps. The crystal data and structure refinements of complexes **1** and **2** are summarized in table 1. Selected bond lengths and angles of complexes **1** and **2** are listed in table 2.

Table 1. Crystal data and structure refinement of **1** and **2**.

| Molecular formula | $C_{25}H_{25}N_3O_2Zn$ | $C_{41}H_{57}N_3O_2Zn$ |
|---|---|---|
| M | 464.85 | 689.27 |
| $T$/K | 293(2) | 293(2) |
| $\lambda$/Å | 0.71073 | 0.71073 |
| Crystal system | Monoclinic | Monoclinic |
| Space group | P21/n | P21/n |
| $a$/Å | 13.0282 | 19.5450(14) |
| $b$/Å | 10.9232 | 10.0947(7) |
| $c$/Å | 14.997(3) | 19.7393(18) |
| $\beta$/° | 96.34(7) | 102.78(3) |
| $V$/Å$^3$ | 2121.1(7) | 3797.8(5) |
| $Z$ | 4 | 4 |
| $F$(000) | 968 | 1480 |
| Reflections collected/unique | 7692/4549 | 8360/8360 |
| Final $R$ indices [I > 2 sigma(I)] | $R1 = 0.0523$, w$R2 = 0.0716$ | $R1 = 0.0943$, w$R2 = 0.2337$ |
| $R$ indices (all data) | $R1 = 0.1484$, w$R2 = 0.0812$ | $R1 = 0.1349$, w$R2 = 0.2475$ |

Table 2. Selected bond lengths (Å) and angles (°) for **1** and **2**.

| | **1** | | |
|---|---|---|---|
| Zn1–O2 | 1.961(3) | Zn1–O1 | 1.962(3) |
| Zn1–N2 | 2.075(3) | Zn1–N1 | 2.078(3) |
| Zn1–N(3) | 2.108(3) | | |
| O2–Zn1–O1 | 94.29(11) | O2–Zn1–N2 | 90.48(13) |
| O1–Zn1–N2 | 150.36(13) | O2–Zn1–N1 | 164.21(13) |
| O1–Zn1–N1 | 89.34(11) | N2–Zn1–N1 | 79.23(14) |
| O2–Zn1–N(3) | 97.63(12) | O1–Zn1–N(3) | 105.30(12) |
| N2–Zn1–N(3) | 103.01(13) | N1–Zn1–N(3) | 96.35(14) |
| | **2** | | |
| Zn1–O1 | 1.952(4) | Zn1–O2 | 1.952(4) |
| Zn1–N1 | 2.068(5) | Zn1–N2 | 2.096(5) |
| Zn1–N(3) | 2.113(5) | | |
| O1–Zn1–O2 | 95.25(18) | O1–Zn1–N1 | 88.61(18) |
| O2–Zn1–N1 | 151.12 | O1–Zn1–N2 | 159.92 |
| O2–Zn1–N2 | 88.13(19) | N1–Zn1–N2 | 79.22 |
| O1–Zn1–N(3) | 98.02 | O2–Zn1–N(3) | 101.12 |
| N1–Zn1–N(3) | 106.72 | N2–Zn1–N(3) | 100.82 |

## 3. Results and discussion

### 3.1. *Crystal study*

The view of the molecular structures of complexes **1** and **2** and their atomic numbering are shown in figures 1 and 2, respectively.

The X-ray analysis of the complexes establishes that in the mononuclear complex, Schiff-base ligand serves as a doubly negative quadridentate ligand. The hydroxyl group in the complex is deprotonated and coordinated [26]. The complexes are five-coordinate, distorted square pyramids in conformity with coordination of Zn(II) to Schiff-base ligands. The ligand occupies the basal plane while pyridine occupies the apical position [23]. The fact that Zn atoms in **1** and **2** are, respectively, 0.30 and 0.35 Å above the plane formed by the $N_2O_2$ coordination supports the supposition that five-coordinate geometry is preferred. The zinc ion is bonded to the oxygen and nitrogen donor atoms of two bidentate ligands.

The Zn–N (py) distance in **1** (2.108(3) Å) is longer than the Zn–N (ligand) distance (2.078(3) Å). The same trend is observed for the bonds to nitrogen in **2**. The Zn–N(ligand) distance is close to what observed in pyrazolyborate complexes of zinc (2.031 Å) [27, 28].

All molecular conductors or semiconductors have a common solid structure feature (i.e. intermolecular $\pi$–$\pi$ stacking interactions) [29–31]. The $\pi$–$\pi$ stacking interactions are also observed in chsa-Zn-pyridine. Each pyridyl ring in chsa-Zn-pyridine molecule stacks together with a pyridyl ring in adjacent molecules by $\pi$–$\pi$ interactions. The interaction continues to the next molecule, resulting in the formation of a one-dimensional molecular chain (figure 1(b)). The chains extend in the crystallographic *c* direction. The intermolecular $\pi$–$\pi$ interaction distance is 3.3 Å. The intermolecular $\pi$–$\pi$ interactions suggest that chsa-Zn-pyridine can possess charge transport properties like $Gaq_3$ [32], which is essential for an electroluminescent material.

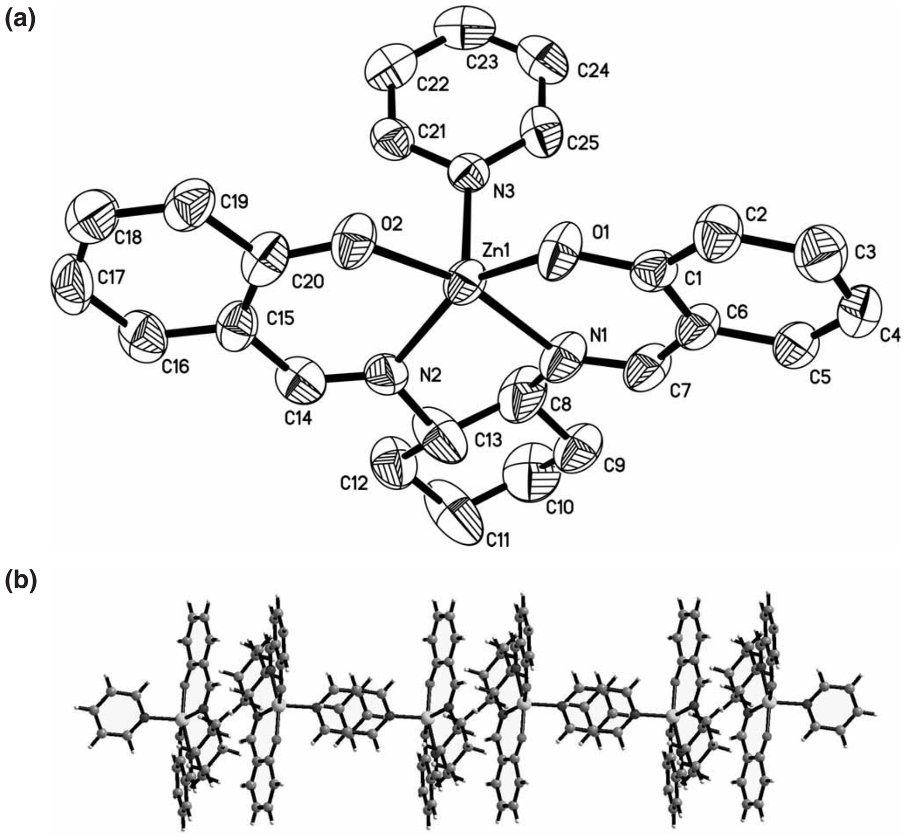

Figure 1. (a) ORTEP view of **1**, with hydrogen atoms omitted for clarity; thermal ellipsoids are drawn at the 50% probability level. (b) A view of the packing of **1** along the *C*-axis.

The other very interesting feature of the crystal structure of **1** is that every two molecules of the complex are situated inversely in the solid state, as shown in figure 1(b). Two molecules are attracted to each other, indicating that there are electronic interactions between the two molecules in the solid state. Two types of C–H···O hydrogen bonds between the chsa-Zn-pyridine oxygen and the adjacent chsa-Zn-pyridine hydrogen were observed in figure 1(b). These are the contacts between $C_{13}$–H, $C_{23}$–H hydrogens and the ligand-oxygen atom ($O_2$), ($O_1$) of the adjacent molecules at 2.594 and 2.592 Å, respectively. They are clearly within the sum of the van der Waals radii for hydrogen (1.2 Å) and oxygen (1.5 Å) [33]. There are weak C–H···O hydrogen bonding interactions between adjacent molecules [32, 34].

Complex **2** exhibits another interesting lattice structure assisted through weak interactions of the type C–H···$\pi$ and $\pi$–$\pi$ (figure 2(b)). In the lattice, each molecule is linked with two other molecules along the crystallographic *c* direction with significant C–H···$\pi$ interactions between phenolic rings of adjacent molecules [35]. The C–H···$\pi$ interactions result from the methyl group of one phenolic ring and the C(1A)–C(2A)–C(3A)–C(4A)–C(5A)–C(6A) ring of the other phenol ring, the edge-to-face separation

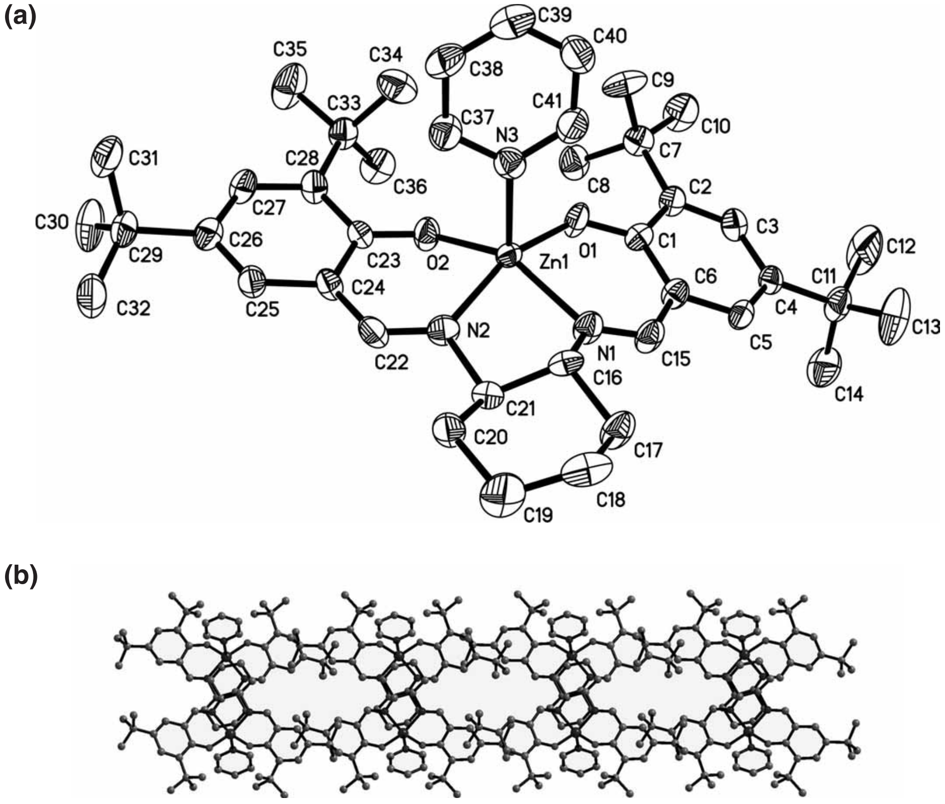

Figure 2. (a) ORTEP view of **2**, with hydrogen atoms omitted for clarity; thermal ellipsoids are drawn at the 50% probability level. (b) Packing diagram of **2** showing channels with dimensions 10.9 × 6.9 Å.

is about 3.79 Å. Thus chains stack to result in large size ellipse cavities with dimensions 10.9 × 6.9 Å with strong $\pi$–$\pi$ stacking interactions between rings of different molecules along the crystallographic *a* direction; the face-to-face distance is about 3.55 Å. These cavities can be observed as channels when the stacking of molecules in the lattice is viewed in the third dimension as shown in figure 2(b). Complex **2** can also be used as an electroluminesent material because its intermolecular $\pi$–$\pi$ interactions give charge transport properties.

### 3.2. *UV-Vis and spectroscopy study*

UV-Vis spectra of the complexes were measured in their solid states. Figure 3 shows the absorption spectra of **1** and **2** in the solid state. The complexes exhibit two absorption bands in the range of 200–500 nm. Complex **1** has two peaks at 245 nm and 355 nm. A red shift is observed in the UV absorption spectrum of **2**, 260 nm and 414 nm. These absorptions are assigned to ligand–ligand charge transfer, which has been confirmed by theoretical study. The red shift may be attributed to the presence of the four tert-butyl groups in **2**, which acts as an auxochrome. Upon UV excitation at 355 nm and 414 nm, solutions of **1** and **2** exhibit intense fluorescence with maxima at 454 nm, 480 nm, respectively. Figure 4 shows the fluorescence spectra of complexes **1**, **2**

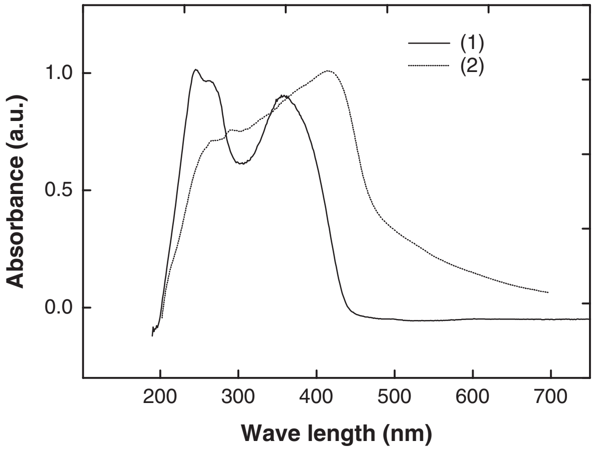

Figure 3. The solid state absorption spectra of complexes **1** and **2**.

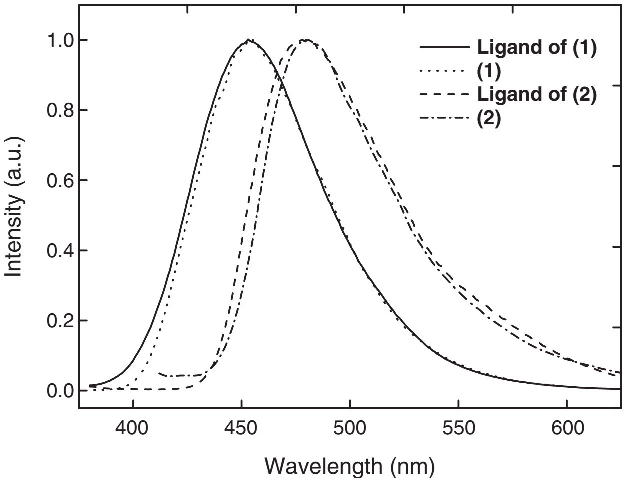

Figure 4. The solid state fluorescence spectra of complexes **1**, **2** and their ligands in DMSO.

and their ligands obtained from DMSO with the excitation at the absorption maximum. The maximal PL peaks of these complexes are identical with those of their ligands, suggesting that the same type excitations and energy bands can be involved in the two molecules [36]. In other words, the emission of the five-coordinate complexes originates from electronic $\pi$–$\pi^*$ transitions within their ligands. The intense emission band suggests that incorporation of zinc increases emission efficiency. Fluorescence properties of other complexes and their OEL properties are now under investigation.

### 3.3. *Electrochemical studies*

The electrochemical properties are investigated in order to determine the effects of the tert-butyl on the redox properties of the complexes. The five-coordinate complexes have

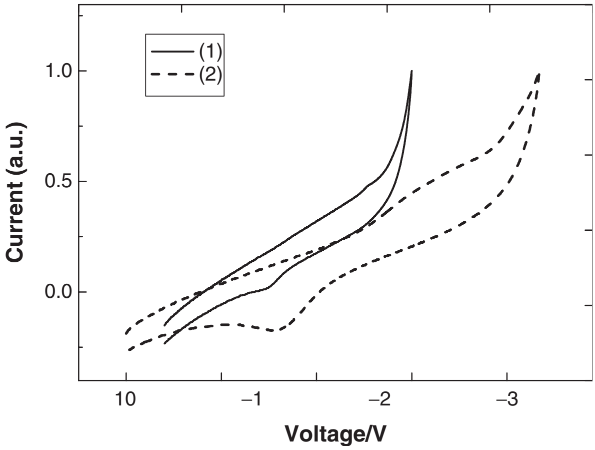

Figure 5. The CV curves of **1** and **2**.

an irreversible oxidative and reductive process in the range of 0 to −3.5 V [37], as shown in figure 5. The reduction peak positions shift from complex **2** (−1.96 V) to complex **1** (−1.46 V) and the oxidative peak positions shift from complex **2** (−0.32 V) to complex **1** (−0.47 V), indicating that electron affinity of the complexes decreases from complex **2** to complex **1**. Therefore, the complexes have lower electron injection energy barriers and easily accept and transport electrons.

### 3.4. *The frontier molecular orbitals of the ground states*

The electrons of a molecule residing in the frontier orbitals are least bound to the molecule and thus are most related to the charge transport properties of the material. The ground state properties of the frontier molecular orbitals and the effect of charge addition on the electronic structure are investigated with the assistance of quantum chemical calculations. In figure 6, we plotted the highest occupied molecular orbital (HOMO) and lowest unoccupied molecular orbital (LUMO) for **1** and **2**. It has been found that the highest occupied orbital is located on the phenolate side and the lowest unoccupied orbital is located on the pyridyl side both in **1** and **2**, which largely preserves the electronic characteristic of their individual ligands without the contribution from Zn. Thus similar spectral properties are expected, as proved by experimental values later and our previous work with other organometallic luminescent complexes [38]. This provides proof that these complexes are typical ligand-centred luminescent complexes.

### 3.5. *Absorption spectra with TD-B3LYP*

Time dependent density functional theory (TD-DFT) calculations have recently been carried out to investigate the electronic properties of cyclometalated Ir and Pt complexes [39, 40]. TD-DFT results are quite accurate for some organic molecules. For quantitative comparison of calculated absorption wavelength with experimental values and to understand the red shift in the experimental absorption spectra of **1** and **2**, we performed spectrum calculations with the (TD-DFT) method.

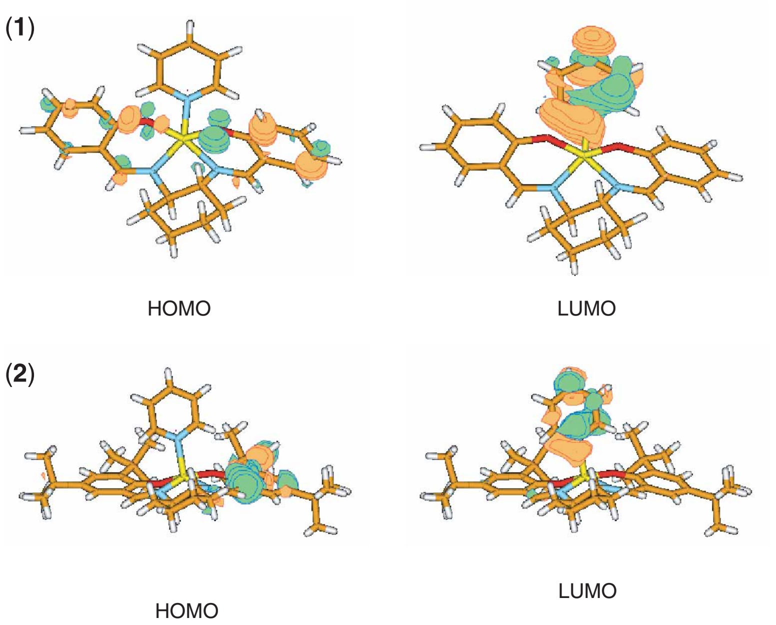

Figure 6. Frontier molecular orbitals of complexes **1** and **2**.

Table 3. The absorption spectrum with TD-B3LYP (nm) and HOMO and LUMO energy (eV).

| | Absorption peak (nm) | | | | |
|---|---|---|---|---|---|
| | TD-DFT | Exp | HOMO (eV) | LUMO (eV) | Energy gap (eV) |
| **1** | 376 | 355 | −4.68 | −1.38 | 3.30 |
| **2** | 450 | 414 | −4.60 | −1.34 | 3.26 |

The absorption spectra of **1** and **2** with TD-B3LYP (nm) and their HOMO and LUMO energies (eV) are listed in table 3. As one can see, the absorption spectra of **1** and **2** calculated with the TD-DFT method predict absorptions at 376 and 450 nm, respectively, which are in good agreement with the experimental values of 355 and 414 nm in solid. The lowest energy excitations ($S_0 \rightarrow S_1$) for **1** and **2** are mainly HOMO → LUMO. However, a red shift of 59 nm displayed for **2** relative to that of **1** is observed. From table 3, it can be attributed to electron-donating substituents residing on the phenolate side, such as tert-butyl of **2**, increase the HOMO energy level (0.08 eV) and the LUMO energy level (0.04 eV), and then decrease the HOMO → LUMO energy gap (0.04 eV) in comparison to that of **1**. As a result, the absorption spectrum of **2** is red shift compared to **1**.

## 4. Conclusions

The crystal structures of **1** and **2** exhibit a number of $\pi$–$\pi$ stacking interactions and hydrogen bond interactions. The presence of intermolecular and hydrogen bond interactions plays an important role in stabilization of the whole structure. From the structure of **1**, it can be seen that two molecules are inverse symmetry, and attract each other by $\pi$–$\pi$ stacking and hydrogen bonding interactions. There are also $\pi$–$\pi$ stacking interactions in the structure of **2**. These all indicate that complexes **1** and **2** may be used as electroluminescent materials. The electrochemical properties of the complexes are sensitive to the tert-butyl substituents, which also affect the electron affinity of the complexes. The experimental and theoretical studies of the absorption spectra of the complexes show that different substitutions have different effects on molecular absorption spectra.

## Supplementary material

Full crystallographic details have been deposited with Cambridge Crystallographic Data Centre for structure **1** (CCDC 225980) and structure **2** (CCDC 225981). These data may be obtained, on request, from The Director, CCDC, 12 Union Road, Cambridge CB2 1EZ, UK (fax: +44-1223-336033; email: deposit@ccdc.cam.ac.uk, www: http://www.ccdc.cam.ac.uk).

## Acknowledgements

This work was supported by the National Natural Science Foundation of China (50225313), the Major State Basic Research Development Program (2002CB613401) and the Youth Fund of Northeast Normal University (No. 111435000).

## References

[1] H. Schiff. *Ann.*, **3**, 343 (1864).
[2] M.A. Ali, R. Bose. *J. Inorg. Nucl. Chem.*, **39**, 265 (1977).
[3] M.F. Iskander, M.M. Mishrikey, L. EL-Sayed, A. El-Toukhy. *J. Inorg. Nucl. Chem.*, **39**, 265 (1977).
[4] G. Davies, N. Kady, M.A.E. Sayed, A. Touhky. *Inorg. Chim. Acta*, **149**, 31 (1988).
[5] P.G. Cozzi. *Chem. Soc. Rev.*, **33**, 410 (2004).
[6] P.G. Cozzi, L.S. Dolci, A. Garelli, M. Montalti, L. Prodi, N. Zaccheroni. *New J. Chem.*, **27**, 692 (2003).
[7] G.A. Morris, H. Zhou, C.L. Stern, S.T. Nguyen. *Inorg. Chem.*, **40**, 3222 (2001).
[8] M. Bandine, P.G. Cozzi, A. Umani-Ronchi. *Chem. Commun.*, **919** (2002) and references therein.
[9] L. Canali, D.C. Sherrington. *Chem. Soc. Rev.*, **28**, 85 (1999).
[10] N.Y. Ito, T. Katsuki. *Bull. Chem. Soc. Jpn.*, **72**, 603 (1999).
[11] T. Katsuki. *Curr. Org. Chem.*, **5**, 663 (2001).
[12] Y.Z. Shen, Y.P.L.Y. Wang, G.D.X.P. Jin, X.Y. Huang, H.W. Hu. *J. Organ. Chem.*, **590**, 242 (1999).
[13] J. Kratamar-Smogrovic, M. Blahova, V. Kettmann. *Chirality*, **3**, 503 (1991).
[14] R.F. Zabinski, M.D. Toney. *J. Am. Chem. Soc.*, **123**, 193 (2001).
[15] Y. Bkouche-Waksman, J.M. Barbe, A. Kvick. *Acta Crystallogr. Sect. B*, **44**, 595 (1988).
[16] S.D. Wetmore, D.M. Smith, L. Radom. *J. Am. Chem. Soc.*, **123**, 8678 (2001).
[17] D. Sattari, E. Alipour, S. Shriani, J. Amighian. *J. Inorg. Biochem.*, **45**, 115 (1992).
[18] T.M. Aminabhavi, N.S. Biradar, S.B. Patil, V.L. Roddabasanagoudar. *Inorg. Chim. Acta*, **107**, 231 (1985).
[19] G. Plesch, C. Friegel, O. Svajlenova, J. Kratsmar-Smogrovic, D. Mlynarcik. *Inorg. Chim. Acta*, **151**, 139 (1988).
[20] C. Gruning, H. Schmidt, D. Rehder. *Inorg. Chem. Commm.*, **2**, 57 (1999).
[21] Y.H. Amada, T. Sano, M. Fujita, T. Fuji, Y. Nishio, K. Shibata. *Chem. Lett.*, **905**, (1993).
[22] C.W. Tang, S.A.Vanslyke. *Appl. Phys. Lett.*, **51**, 913 (1987).
[23] A.L. Singer, D.A. Atwood. *Inorg. Chim. Act.*, **277**, 157 (1998).

[24] M.D. Halls, H.B. Schligel. *Chem. Mater.*, **13**, 2632 (2001).

[25] G.M. Sheldrick. *SHELXS97*, *Program for Crystal Structure Refinement*, University of Göttingen, Göttingen, Germany (1997); G.M. Sheldrick. *SHELXL97*, *Program for Crystal Structure Solution*, University of Göttingen, Göttingen, Germany (1997).

[26] X. Wang, X.M. Zhang, H.X. Liu. *Polyhedron*, **142**, 293 (1995).

[27] K.W. Yang, Y.Z. Wang, Z.X. Huang. *Polyhedron*, **16**, 109 (1996).

[28] C. Kimblin, G. Parkin. *Inorg. Chem.*, **35**, 6921 (1996).

[29] A. Kobayashi, H. Kim, Y. Sasaki, K. Murata, R. Kato, H. Kobayashi. *J. Chem. Soc.*, *Faraday Tran.*, **86**, 361, (1990).

[30] K. Takahashi, T. Shirahata, K.J. Tomitani. *Mater. Chem.*, **7**, 2375, (1997).

[31] X.C. Li, H. Sirringhaus, F. Garnier, A.B. Holmes, S.C. Moratti, N. Feeder, W. Clegg. *J. Am. Chem. Soc.*, **120**, 2206 (1998).

[32] Y. Wang, W.X. Zhang, Y.Q. Li, L.Ye, G.D. Yang. *Chem. Mater.*, **11**, 530 (1999).

[33] A.J. Bondi. *Phys. Chem.*, **68**, 441 (1964).

[34] A.K. Sah, C.P. Rao, P.K. Saarenketo, E. Kolehmainen. *Carbohydrate Research*, **335**, 33 (2001).

[35] X.L. Wang, C. Qin, E.B. Wang, L. Xu, Z.M. Su, C.W. Hu. *Angew. Chem. Int. Ed.*, **43**, 5036 (2004).

[36] Y.Q. Li, Y. Liu, W.M. Bu, D. Lu, Y. Wu, Y. Wang. *Chem. Mater.*, **12**, 2672 (2000).

[37] G. Wang, F.S. Liang, Z.Y. Xie, G.P. Su, L.X. Wang, X.B Jing, F.S. Wang. *Synthetic Metals*, **131**, 1 (2002).

[38] Z.M. Su, H.Z Gao, H. Cheng, B. Chu, L.H. Chen, R.S. Wang, Y. Wang, J.C. Shen. *Science in China* (*Series B*), **43**, 657 (2000).

[39] P.J. Hay. *Phys. Chem. A.*, **106**, 1634 (2002).

[40] A.B. Tamayo, B.D. Alleyne, P.I. Djurovich, S.I. Lamansky, I. Tsyba, N.N. Oh, R. Bau, M.E. Thompson. *J. Am. Chem. Soc.*, **125**, 7377 (2003).